Thermodynamic Properties of Tetra-*n*-butylammonium and Tetra-*n*-butylphosphonium Hydroxycarboxylate Semiclathrate Hydrates

Kazuhiro Minamikawa[1,2], *Jin Shimada*[1,2,3], *Takeshi Sugahara*[1,2,*], *Takayuki Hirai*[1,2]

[1]Division of Chemical Engineering, Department of Materials Engineering Science, Graduate School of Engineering Science, Osaka University, 1-3 Machikaneyama, Toyonaka, Osaka, 560-8531, Japan

[2]Division of Energy and Photochemical Engineering, Research Center for Solar Energy Chemistry, Graduate School of Engineering Science, Osaka University, 1-3 Machikaneyama, Toyonaka, Osaka, 560-8531, Japan

[3]Research Fellow of Japan Society for the Promotion of Science, 5-3-1 Kojimachi, Chiyoda-ku, Tokyo 102-0083, Japan

KEYWORDS: semiclathrate hydrate, phase equilibria, enthalpy, thermal storage material

ABSTRACT

Semiclathrate hydrate (SCH) has been expected to be one of the phase change materials suitable for cold energy storage. In the present study, the equilibrium temperature, dissociation enthalpy, and crystal structure of tetra-*n*-butylammonium(TBA)-Tar, tetra-*n*-butylphosphonium(TBP)-Tar, and TBA-Mala SCHs were investigated, where the hydroxycarboxylate anions were malate (-Mala) and tartarate (-Tar). The maximum equilibrium temperature of each SCH system at the stoichiometric composition was (279.54±0.05) K for TBA-Tar SCH, (275.44±0.05) K for TBP-Tar SCH, and (278.69±0.05) K for TBP-Mala SCH at atmospheric pressure. Each dissociation enthalpy was (172±3) $kJ \cdot kg^{-1}$ for TBA-Tar SCH, (161±3) $kJ \cdot kg^{-1}$ for TBP-Tar SCH, and (172±3) $kJ \cdot kg^{-1}$ for TBP-Mala SCH. The SCHs with hydroxy group(s) in the anion of onium salts are more environmentally-friendly than SCHs with halide anion. The environmentally-friendly SCHs measured in the present study could be used as refrigerants in the logistics of vegetables and fruits because the equilibrium temperature is suitable to preserve their freshness.

1. INTRODUCTION

Unused thermal energy has been released from various energy-consuming points, such as vehicles, life, and factories, to environment. Phase change materials (PCMs) have abilities not only to store the unused thermal energy but also to contribute to filling the gap between electric power generation and demand. Ice is known as one of the famous PCMs, whereas the melting temperature of ice is too low for storage of vegetables, fruits[1] and vaccines[2,3]. So that, it is essential to develop the PCMs with phase change temperatures suitable for various cold chains, instead of ice.

Semiclathrate hydrate (SCH) or ionic clathrate hydrate is a promising candidate as a PCM. SCH is a crystalline inclusion compound consisting of host water molecules and appropriate guest substance. Tetra-*n*-butylammonium (TBA) and tetra-*n*-butylphosphonium (TBP) salts have been investigated as typical guest substances. The cations are enclathrated in polyhedral cages and the anions form hydrogen-bonded networks with the host water molecules[4-7]. One of the well-investigated SCHs is tetra-*n*-butylammonium bromide (TBAB) SCH. TBAB SCH with the hydration number of 26 has the relatively large dissociation enthalpy (192±3 $kJ \cdot kg^{-1}$)[8]. Taking account of its characteristics, TBAB SCH slurry was introduced to the shopping mall and office in Japan as air-conditioning media[9].

Thermodynamic properties of SCH depend on the combination of cations with anions[10-13]. Generally speaking, the phosphonium cation decreases the equilibrium temperature of SCH compared to the ammonium cation with the same alkyl chains as the phosphonium one. Thermodynamic properties of SCHs are suitable for PCMs in cold chains, because of not only the equilibrium temperatures within 270 to 300 K at atmospheric pressure but also the relatively large dissociation enthalpies (160−220 $kJ \cdot kg^{-1}$).[8,14-24] According as the working temperatures of PCMs

needed in cold chains, to develop SCHs with various equilibrium temperatures is required. For example, SCHs with the equilibrium temperatures of 280 to 283 K are suitable for storage of vegetables and fruits,[1] 275 to 281 K for vaccines, [2,3] 278 to 288 K for air conditioning,[24] and 288 to 308 K for cooling of lithium-ion battery[25]. In the temperature range needed in cold chains, especially, a repertoire of SCHs with the equilibrium temperatures around 275 to 283 K is relatively small[10,11,19,26-31].

We focused on the SCH systems with dicarboxylate anions. The maximum equilibrium temperatures of TBA-Oxalate, TBA-Malonate, and TBA-Succinate SCHs were reported to be 289.7 K[26], 287.5 K[26], and 286.1 K[10] at atmospheric pressure, respectively. Engineering a way to develop SCHs with an equilibrium temperature of 275 to 283 K has gained considerable interests. Muromachi et al. [28,29] reported that, when the hydroxy group is introduced to a carboxylate anion, the replacement of water molecules with the oxygen atoms in hydroxy groups makes the equilibrium temperature decreases. In the present study, the thermodynamic properties of tetra-*n*-butylammonium hydroxycarboxylate (TBA-HDC) and tetra-*n*-butylphosphonium hydroxycarboxylate (TBP-HDC) SCHs were investigated. As hydroxycarboxylate (HDC) anions, succinate (-Suc), malate (-Mala), and tartarate (-Tar) were used. The chemical structures of HDC used in the present study were shown in **Figure 1**.

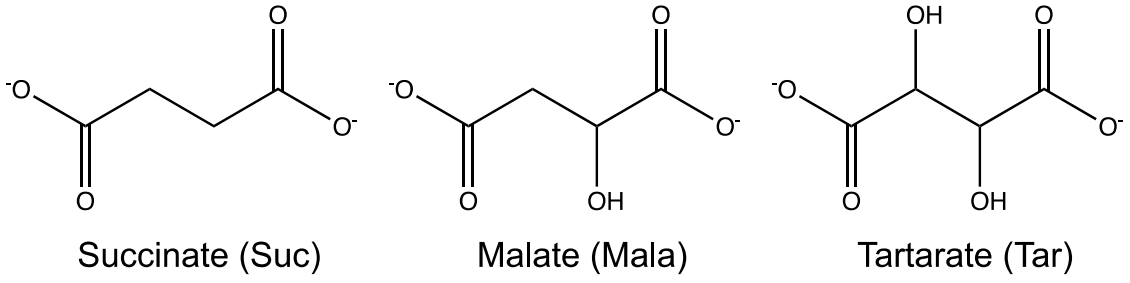

Figure 1. Chemical structures of the hydroxycarboxylate anions used in the present study.

2. Experimental section

2.1 Materials

The chemicals used in the present study are listed in **Table 1**. TBA-HDC and TBP-HDC salts were synthesized by neutralization reaction of tetra-*n*-butylammonium hydroxide or tetra-*n*-butylphosphonium hydroxide with the corresponding hydroxycarboxylic acids in the aqueous solution. Neutralization reactions were performed for 24 hours. The products were confirmed by ^{1}H and ^{13}C nuclear magnetic resonance (NMR, JEOL, ECS-400). The NMR results were summarized in the supporting information. NMR results showed no impurity-derived signals or anomalies in the integral ratio. The purity of the synthesized TBA-HDC and TBP-HDC were equal to or higher than that originally contained in the synthesis reagents.

Table 1. Information on Chemicals Used in the Present Study.

chemical name	CAS reg. no.	source	mass fraction purity	molecular (formula) weight
tetra-*n*-butylammonium hydroxide($C_{16}H_{37}NO$)	2052-49-5	Tokyo Chemical Industry Co., Ltd.	0.415 mass fraction in aqueous solution	259.48
tetra-*n*-butylphosphonium hydroxide($C_{16}H_{37}PO$)	14518-69-5	Tokyo Chemical Industry Co., Ltd.	0.405 mass fraction in aqueous solution	276.44
(L)-tartaric acid($C_4H_6O_6$)	87-69-4	Tokyo Chemical Industry Co., Ltd.	>0.990	150.09
(L)-malic acid($C_4H_6O_5$)	97-67-6	Tokyo Chemical Industry Co., Ltd.	>0.980	134.09
succinic acid($C_4H_6O_4$)	110-15-6	Tokyo Chemical Industry Co., Ltd.	>0.990	118.09
water(H_2O)	7732-18-5	distilled	resistivity is 0.46 MΩ cm	18.02

2.2 Apparatus and procedures

Approximately 1 cm^3 of aqueous solutions were prepared at different compositions from x = 0.0018−0.0229 (w = 0.061−0.452) for TBA-Tar, x = 0.0018−0.0191 (w = 0.062−0.419) for TBP-Tar, x = 0.0030−0.0208 (w = 0.099−0.434) for TBP-Mala using electric balance (SHIMADZU, AUW220D) with an uncertainly of 0.2 mg. The symbols x and w represent the mole and mass fractions, respectively. The SCHs were formed in glass vials at 263 K. The vials for TBA-Tar SCH were put into a water bath thermostated with a cooling water circulator at 275 K (Taitec, CL-80R or EYELA, NCB-3100). The vials for TBP-Tar and TBP-Mala SCHs were put into a propylene glycol bath thermostated with a cooling water circulator at 270 K (Taitec, CL-80R or EYELA,

NCB-3100). The system temperature was increased by a step of 0.1 K. The temperature was maintained for at least 4 h at each temperature with frequently stirring the samples. The temperature at which SCH completely dissociated was measured as an equilibrium temperature. The system temperature was measured with a thermistor thermometer (Takara, D632, reproducibility: 0.02 K. The probe was calibrated with a Pt resistance thermometer defined by ITS-90). The maximum uncertainty of equilibrium temperature was 0.05 K.

The hydration numbers (n) of TBA-Tar, TBP-Tar and TBP-Mala SCHs were estimated from the stoichiometric compositions. To determine the stoichiometric compositions, the apparent dissociation enthalpy (per mass of aqueous solution, not per mass of SCH) at each composition was measured using a micro differential scanning calorimeter (DSC) (Setaram, μDSC VIIevo). Apparent dissociation enthalpy reaches the maximum value at stoichiometric composition[20,23,31,32] because either excess amount of water or guest salt remains at a composition except for the stoichiometric composition. We prepared approximately 20 mg of TBA-HDC or TBP-HDC aqueous solutions for DSC measurements. The sample mass was precisely measured with electric balance (A&D, BM-22) with an uncertainty of 0.02 mg. The furnace temperature was decreased to 248 K at a cooling rate of 0.5 $K \cdot min^{-1}$. After the SCH formation, to remove metastable structures from the sample, the formed SCH was repeatedly annealed while partially dissociated[33]. After the peaks derived from metastable structures disappeared completely, the furnace temperature was decreased to 248 K again and then increased from 248 K to the desired temperature at a heating rate of 0.02 $K \cdot min^{-1}$. We calibrated the DSC with a dedicated Joule heat calibrator (Setaram, EJ3). In addition, water was adopted as a reference. The dissociation enthalpy of water ice was in good agreement with the reference within an uncertainty less than 2 $kJ \cdot kg^{-1}$. We have reported the

dissociation enthalpies measured with the same DSC[11-13,19,22,23,31,32]. The overall uncertainty in the dissociation enthalpy measured in the present study is less than 3 $kJ \cdot kg^{-1}$.

The crystal structures of TBA-HDC SCH and TBP-HDC SCH were estimated by powder X-ray diffraction (PXRD). To compare the crystal structures of SCH, we measured the PXRD pattern of TBA-Suc and TBA-Mala SCHs as well as that of TBA-Tar, TBP-Tar, and TBP-Mala SCHs. The samples for PXRD measurement were prepared from aqueous solutions with the stoichiometric compositions. The PXRD sample was crystallized in a freezer kept at 263 K and then we annealed the samples well. The PXRD patterns were measured at 150 K and atmospheric pressure by use of a diffractometer (PANalytical, X'Pert-MPD) with a cold stage (Anton Paar, TTK450) and Cu Kα X-ray (45 kV, 40 mA). The PXRD measurements were performed in the step scan mode with a scan rate of $2.7° \cdot min^{-1}$ and a step size approximately 0.02°. PXRD pattern indexing and cell refinement were carried out using the Chekcell[34] and PowderX[35] programs.

3. RESULTS AND DISCUSSION

3.1. Phase Equilibrium Relations.

Phase equilibrium relations (temperature T and composition x) of TBA-Tar, TBP-Tar, and TBP-Mala SCHs obtained by the visual observation method were shown in **Figure 2** and summarized in **Tables 2-4**. The phase diagrams of TBA-Tar, TBP-Tar, and TBP-Mala SCHs exhibited a congruent-type phase behavior, which is typical in SCHs. The maximum equilibrium temperature of TBA-Tar SCH was (279.54±0.05) K at x_1= (0.0162±0.0005) (n = 61±1). The maximum equilibrium temperatures of TBA-Mala SCH and TBA-Suc SCH were reported to be 284.2 K at

x_1= 0.0156 (n = 63±1)[26] and 286.1 K at x_1= 0.0157 (n = 62.6±0.6)[10], respectively. The maximum equilibrium temperatures of TBP-Tar and -Mala SCHs were (275.44±0.05) K at x_1= (0.0160±0.0001) (n = 62±1) and (278.69±0.05) K at x_1= (0.0157±0.0002) (n = 63±1), respectively. The maximum equilibrium temperature of TBP-Suc SCH was reported to be 282.7 K[13] at x_1= 0.0157 (n = 63±2)[13]. The stoichiometric composition, the hydration number, and the dissociation enthalpy of each SCH were estimated by DSC results as will be described later in **Figures 3 and 4**. The maximum equilibrium temperature of each TBA-HDC SCH was higher than those of corresponding TBP-HDC SCH (**Table 5**). Such trend is due to the distortion of the crystal structure caused by the difference in bond lengths[7] between C−P and C−N and the electrostatic interaction[11] between more positively-charged phosphorus atom in phosphonium cation (than nitrogen atom in ammonium cation) and negatively charged oxygen atoms in surrounding water molecules. These results may be caused by the differences in the electrostatic interactions on dicarboxylate anions with phosphonium or ammonium cations.

The order of maximum equilibrium temperature was TBA-Tar SCH < TBA-Mala SCH < TBA-Suc SCH. The larger number of hydroxy groups in the guest substance makes the equilibrium temperature lowered. This trend was observed in not only TBA-HDC SCH systems but also TBP-HDC SCH ones. The trend was consistent with the literature[28], where the hydroxy group in lactate anion lowered the equilibrium temperature compared to the propionate one.

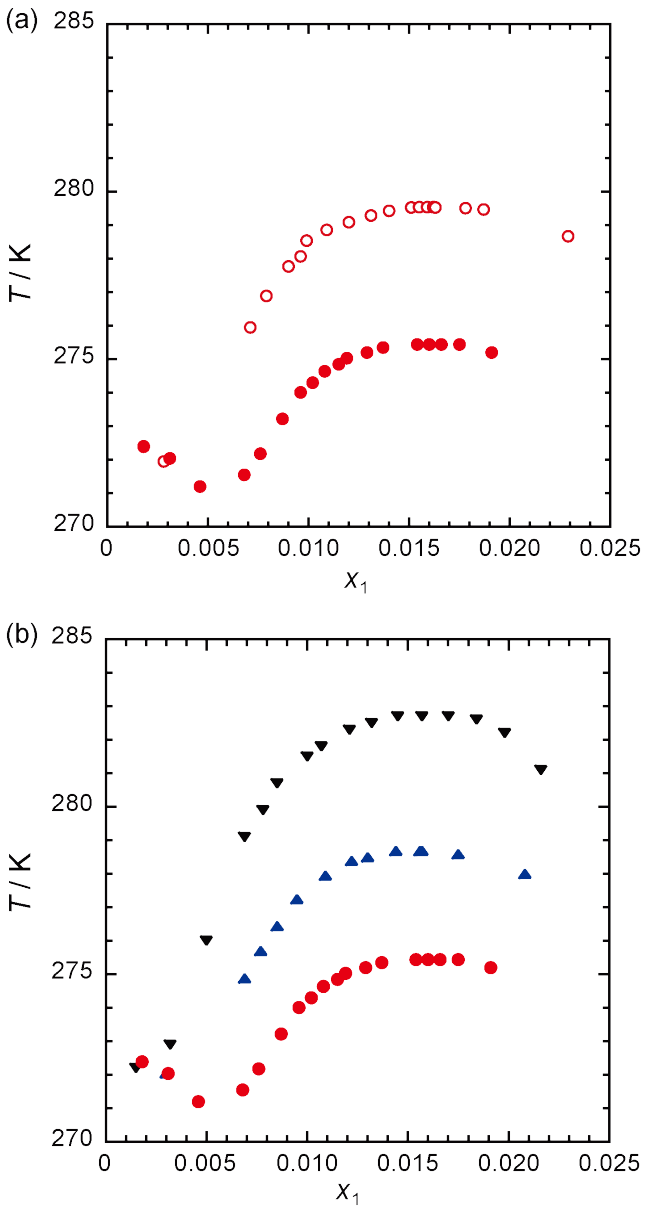

Figure 2. Equilibrium temperature (T)-composition (x) relations of the binary systems at atmospheric pressure. Panel (a), TBA-Tar (1) + water (2) (red open circles, present study) and TBP-Tar (1) + water (2) (red closed circles, present study) systems; Panel (b), TBP-Tar (1) + water (2) system (red closed circles, present study), TBP-Mala (1) + water (2) system (blue triangles, present study) and TBP-Suc (1) + water (2) system (black inverted triangles, ref. 13)

Table 2. Phase Equilibrium Relations of Temperature (T) – Composition (Mass Fraction w_1 and Mole Fraction x_1) at Atmospheric Pressure in the TBA-Tar (1) + Water (2) Binary System.[a] The Symbols H, I, and L stand for Semiclathrate Hydrate, Ice, and Aqueous Solution Phases.

TBA-Tar (1) + water (2)							
w_1	x_1	T / K	phases	w_1	x_1	T / K	phases
0.061	0.0018	272.40	I-L	0.334	0.0140	279.43	H-L
0.090	0.0028	271.95	I-L	0.351	0.0151	279.53	H-L
0.200	0.0071	275.95	H-L	0.355	0.0155	279.54	H-L
0.219	0.0079	276.89	H-L	0.362	0.0159	279.54	H-L
0.242	0.0090	277.77	H-L	0.366[b]	0.0162[b]	279.54[b]	H-L
0.254	0.0096	278.07	H-L	0.368	0.0163	279.53	H-L
0.260	0.0099	278.54	H-L	0.389	0.0178	279.51	H-L
0.280	0.0109	278.86	H-L	0.400	0.0187	279.47	H-L
0.300	0.0120	279.09	H-L	0.452	0.0229	278.67	H-L
0.317	0.0131	279.29	H-L				

[a] Standard uncertainties u are $u(w) = 0.005$, $u(x) = 0.0005$ and $u(T) = 0.05$ K

[b] Maximum equilibrium temperature at stoichiometric composition

Table 3. Phase Equilibrium Relations of Temperature (T) – Composition (Mass Fraction w_1 and Mole Fraction x_1) at Atmospheric Pressure in the TBP-Tar (1) + Water (2) Binary System.[a] The Symbols H, I, and L stand for Semiclathrate Hydrate, Ice, and Aqueous Solution Phases.

TBP-Tar (1) + water (2)							
w_1	x_1	T / K	phases	w_1	x_1	T / K	phases
0.062	0.0018	272.39	I-L	0.301	0.0115	274.85	H-L
0.102	0.0031	272.04	I-L	0.309	0.0119	275.03	H-L
0.147	0.0046	271.20	I-L	0.326	0.0129	275.20	H-L
0.202	0.0068	271.55	H-L	0.340	0.0137	275.35	H-L
0.222	0.0076	272.18	H-L	0.367	0.0154	275.44	H-L
0.245	0.0087	273.22	H-L	0.376[b]	0.0160[b]	275.44[b]	H-L
0.265	0.0096	274.01	H-L	0.384	0.0166	275.44	H-L
0.276	0.0102	274.30	H-L	0.398	0.0175	275.44	H-L
0.288	0.0108	274.64	H-L	0.419	0.0191	275.20	H-L

[a] Standard uncertainties u are $u(w) = 0.002$, $u(x) = 0.0001$ and $u(T) = 0.05$ K

[b] Maximum equilibrium temperature at stoichiometric composition

Table 4. Phase Equilibrium Relations of Temperature (T) – Composition (Mass Fraction w_1 and Mole Fraction x_1) at Atmospheric Pressure in the TBP-Mala (1) + Water (2) Binary System.[a] The Symbols H, I, and L stand for Semiclathrate Hydrate, Ice, and Aqueous Solution Phases.

TBP-Mala (1) + water (2)							
w_1	x_1	T / K	phases	w_1	x_1	T / K	phases
0.099	0.0030	272.05	I-L	0.322	0.0130	278.50	H-L
0.201	0.0069	274.88	H-L	0.346	0.0144	278.69	H-L
0.218	0.0077	275.70	H-L	0.364	0.0156	278.69	H-L
0.236	0.0085	276.44	H-L	0.365[b]	0.0157[b]	278.69[b]	H-L
0.258	0.0095	277.25	H-L	0.391	0.0175	278.59	H-L
0.284	0.0109	277.95	H-L	0.434	0.0208	278.01	H-L
0.308	0.0122	278.40	H-L				

[a] Standard uncertainties u are $u(w) = 0.003$, $u(x) = 0.0002$ and $u(T) = 0.05$ K

[b] Maximum equilibrium temperature at stoichiometric composition

Table 5. Stoichiometric Composition (Mass Fraction w and Mole Fraction x), Hydration Number (n), Dissociation Enthalpy $\Delta_d H$, and Maximum Equilibrium Temperature (T) of SCHs in the TBA-HDC or TBP-HDC (1) + Water (2) System.

Compound		x_1	w_1	n	$\Delta_d H$ / kJ · kg $^{-1}$	T / K
TBA-Suc	present study	0.0159 [a]	0.360 [a]	63 [a]	192 [a]	-
	ref. 10	0.0159	0.360	62.6	-	286.1
	ref. 26	0.0161	0.353	61	-	285.2
TBA-Mala	present study	0.0156 [b]	0.352 [b]	63 [b]	183 [b]	-
	ref. 26	0.0156	0.352	63	-	284.2
TBA-Tar	present study	0.0162 [c]	0.366 [c]	61 [c]	172 [c]	279.54 [c]
TBP-Suc	ref. 13	0.0157	0.360	63	-	282.7
TBP-Mala	present study	0.0157 [d]	0.365 [d]	63 [d]	172 [d]	278.69 [d]
TBP-Tar	present study	0.0160 [e]	0.376 [e]	62 [e]	161 [e]	275.44 [e]

[a] Standard uncertainties u are $u(x) = 0.0003$, $u(w) = 0.005$, $u(n) = 1$, and $u(H) = 3$ kJ·kg^{-1}.

[b] Standard uncertainties u are $u(x) = 0.0007$, $u(w) = 0.009$, $u(n) = 2$, and $u(H) = 3$ kJ·kg^{-1}.

[c] Standard uncertainties u are $u(x) = 0.0005$, $u(w) = 0.005$, $u(n) = 1$, $u(H) = 3$ kJ·kg^{-1}, and $u(T) = 0.05$ K.

[d] Standard uncertainties u are $u(x) = 0.0002$, $u(w) = 0.003$, $u(n) = 1$, $u(H) = 3$ kJ·kg^{-1}, and $u(T) = 0.05$ K.

[e] Standard uncertainties u are $u(x) = 0.0001$, $u(w) = 0.002$, $u(n) = 1$, $u(H) = 3$ kJ·kg^{-1}, and $u(T) = 0.05$ K.

3.2. Dissociation Enthalpy Measured by DSC.

The composition ranges in the DSC measurements were x_1= (0.0146−0.0177 for TBA-Tar SCH, x_1= (0.0146−0.0175) for TBP-Tar SCH, and x_1= (0.0144−0.0170) for TBP-Mala SCH. Typical DSC thermograms of TBA-HDC and TBP-HDC SCHs at a heating rate of 0.02 K/min are shown in **Figure 3**. From the vertices of the apparent dissociation enthalpy curves in **Figure 4**, we determined the stoichiometric compositions and true dissociation enthalpies ($\Delta_d H$) of SCHs[20,23,31,32]. The obtained dissociation enthalpies ($\Delta_d H$) of TBA-HDC and TBP-HDC SCHs are summarized in **Table 5**. The dissociation enthalpy of TBA-HDC and TBP-HDC SCHs was slightly larger than that of non-halide-based SCHs which have equilibrium temperatures close to the TBA-HDC and TBP-HDC SCHs.[13,17,20,29,31,36]

Mala or Tar anions have one or two hydroxy group(s) in anion. The dissociation enthalpies of TBA-Mala and -Tar SCHs were larger than that of TBP-Mala and -Tar SCHs, respectively, whereas the dissociation enthalpy of TBA-Suc SCH (Suc anion has no hydroxy group) was equal to that of TBP-Suc SCH within uncertainty.

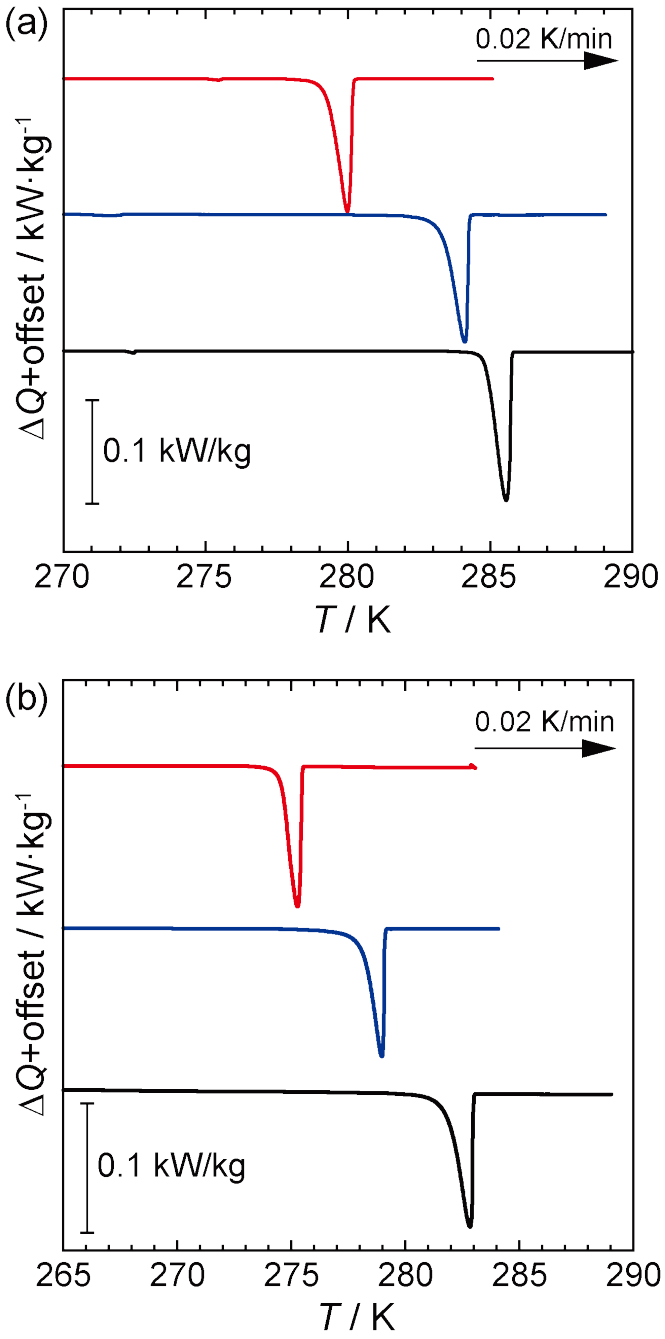

Figure 3. DSC thermograms (heat flow ΔQ, temperature T) at a heating rate of 0.02 K/min. Panel(a), TBA-Tar (red, top); TBA-Mala (blue, middle); TBA-Suc (black bottom). Panel (b), TBP-Tar (red, top); TBP-Mala (blue, middle); TBP-Suc (black, bottom)[13].

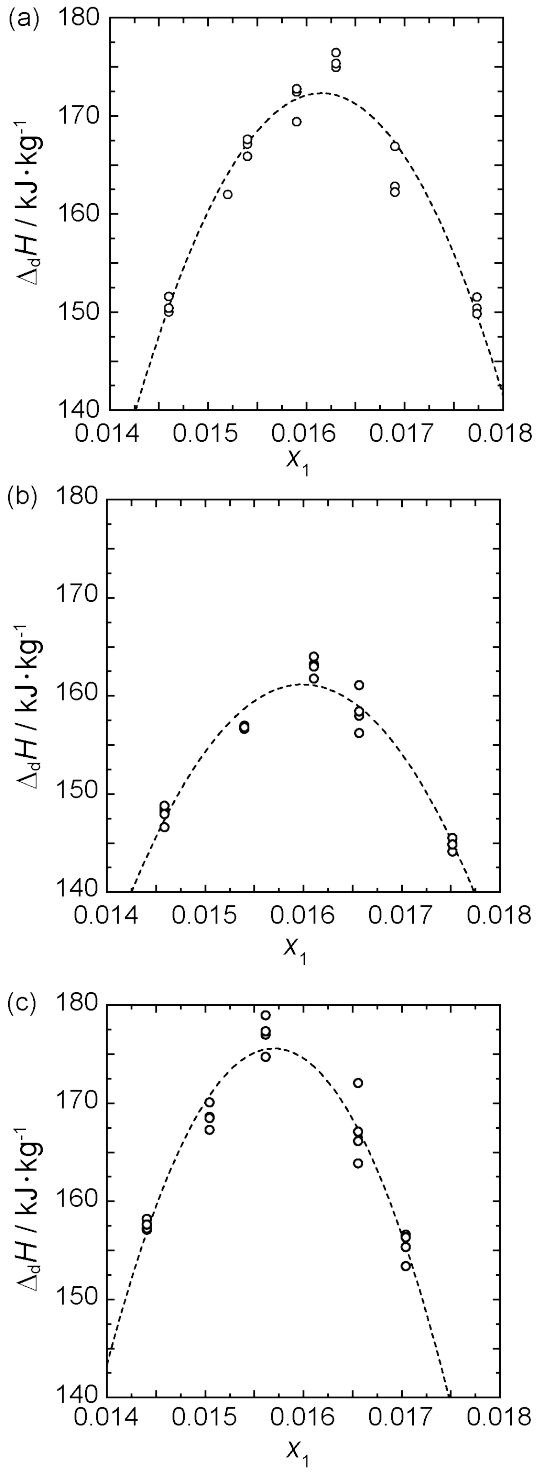

Figure 4. Apparent dissociation enthalpies of (a) TBA-Tar (1) + water (2) system, (b) TBP-Tar (1) + water (2) system, and (c) TBP-Mala (1) + water (2) system

3.3. Powder X-ray Diffraction Profiles of SCHs.

PXRD patterns of TBA-HDC and TBP-HDC SCHs measured at 150 K were shown in **Figures 5 and 6**, respectively. The pattern of TBA-Suc SCH measured in the present study agreed with that (tetragonal, *P*4/*mmm*) reported in the literature,[10] although there was a slight difference caused by different measurement temperatures. TBA-HDC and TBP-HDC SCHs measured in the present study have almost the same tetragonal structure because all of them have similar PXRD patterns. The estimated lattice parameters of TBA-HDC and TBP-HDC SCHs were summarized in **Table 6**.

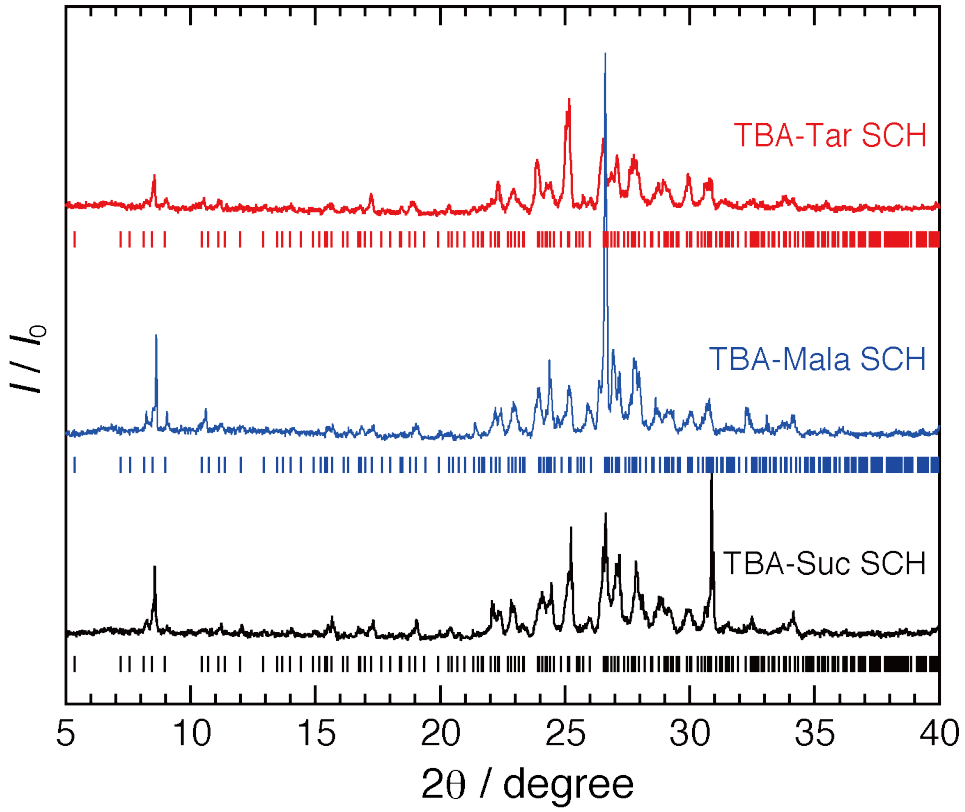

Figure 5. Powder X-ray diffraction (PXRD) patterns of TBA-Tar (red, top), TBA-Mala (blue, middle), and TBA-Suc (black, bottom) SCHs measured at 150 K and atmospheric pressure. The tickmarks indicate reflections from each SCH listed in Table 6.

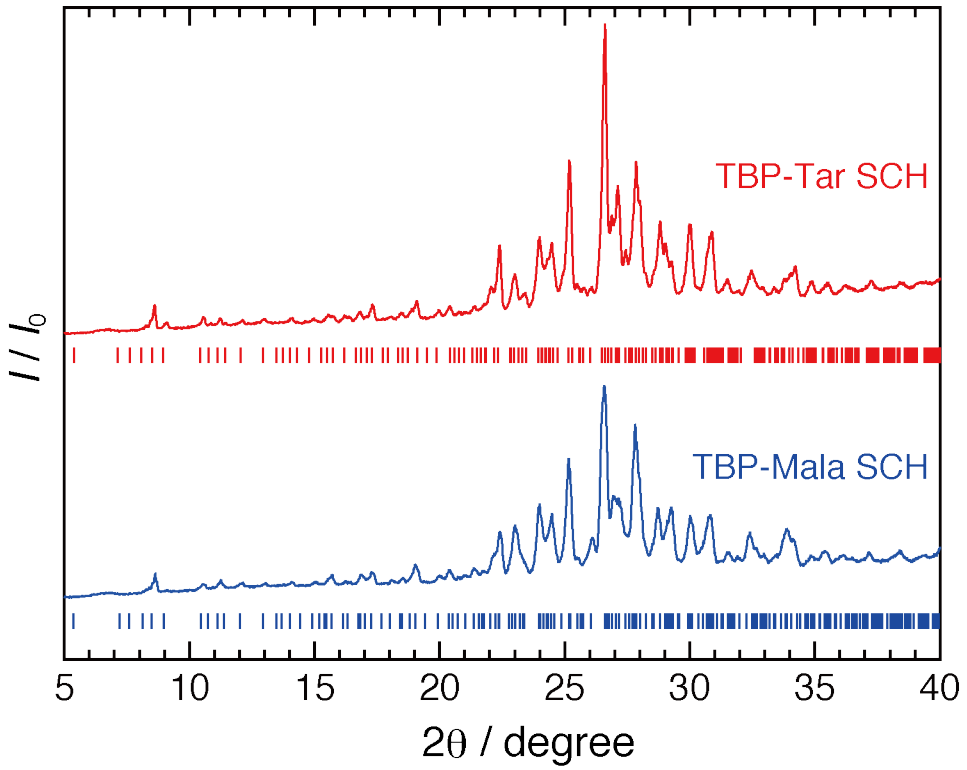

Figure 6. Powder X-ray diffraction (PXRD) patterns of TBP-Tar (red, top) and TBP-Mala (blue, bottom) SCHs measured at 150 K and atmospheric pressure. The tickmarks indicate reflections from each SCH listed in Table 6.

Table 6. Crystal structure and Lattice Parameters of SCHs measured at 150 K in the present study

SCH		crystal structure	lattice parameters	
			a / nm	*c* / nm
TBA-Tar	present study	tetragonal	2.333±0.001	1.228±0.001
TBA-Mala	present study	tetragonal	2.330±0.001	1.227±0.001
TBA-Suc	present study	tetragonal	2.335±0.002	1.228±0.001
	ref. 10	tetragonal	2.36 (at 263 K)	1.26 (at 263 K)
TBP-Tar	present study	tetragonal	2.321±0.001	1.239±0.001
TBP-Mala	present study	tetragonal	2.329±0.001	1.227±0.001
TBP-Suc13	ref. 13	tetragonal	2.359 (at 150 K)	1.247 (at 150 K)

4. CONCLUSION

The purpose in the present study was to explore an environmentally-friendly SCH with an equilibrium temperature from 275 to 283 K. The combination of TBA or TBP cation with hydroxycarboxylate anion was investigated as environmentally-friendly guest onium salts. The maximum equilibrium temperatures of TBA-Tar, TBP-Tar, and TBP-Mala SCHs at atmospheric pressure were (279.54±0.05) K at x_1= (0.0162±0.0005), (275.44±0.05) K at x_1= (0.0160±0.0001), and (278.69±0.05) K at x_1= (0.0157±0.0002), respectively. The dissociation enthalpies of TBA-Tar, TBP-Tar, and TBP-Mala SCHs were (172±3), (161±3), and (172±3) $kJ \cdot kg^{-1}$, respectively. An increase in the number of hydroxy groups led to decrease in the equilibrium temperature. Additionally, the cation replacement of TBA with TBP results in a decrease in the equilibrium temperature. SCH with environmentally-friendly hydroxycarboxylate instead of halide has the potential to be a promising phase change material (PCM) in the transportation of food and pharmaceuticals.

ASSOCIATED CONTENT

Supporting Information

The ^{1}H, ^{13}C, and ^{31}P NMR results of the salts prepared in the present study are summarized in the supporting information. This material is available free of charge on the ACS Publications website at http://pubs.acs.org.

AUTHOR INFORMATION

Corresponding Author

*(T.S.) Tel and Fax: +81-6-6850-6293. E-mail: sugahara.takeshi.es@osaka-u.ac.jp.

ORCID

Jin Shimada: 0000-0002-9720-5963

Takeshi Sugahara: 0000-0002-5236-5605

Takayuki Hirai: 0000-0003-4747-4919

Funding

This work was supported by JSPS KAKENHI Grant-in-Aid for JSPS Fellows (JP21J20788 and JP22KJ2069 for J.S.) and Grant-in-Aid for Scientific Research (JP22K05050 for T.S.).

Notes

The authors declare no competing financial interest.

ACKNOWLEDMENTS

The authors acknowledge scientific support from the Gas-Hydrate Analyzing System (GHAS) of the Division of Chemical Engineering, Department of Materials Engineering Science, Graduate School of Engineering Science, Osaka University. KM also acknowledges fruitful discussion in

the researcher meeting “The H2O Science 2022”, supported by the Institute of Low Temperature Science, Hokkaido University.

References

1) Xu, X.; Zhang, X. Simulation and experimental investigation of a multi-temperature insulation box with phase change materials for cold storage, *J. Food Eng.* **2021***, 292*, 110286. DOI: 10.1016/j.jfoodeng.2020.110286

2) Davis, H.; Dow, T.; Isopi, L.; Blue, J. T. Examination of the effect of agitation on the potency of the Ebola Zaire vaccine rVSVΔG-ZEBOV-GP, *Vaccine* **2020**, *38*, 2643−2645. DOI: 10.1016/j.vaccine.2020.02.002

3) American Hospital Association, Special Bulletin, COVID-19 vaccine storage requirement, 2021. https://www.aha.org/system/files/media/file/2021/03/aha-releases-covid-19-vaccine-storage-requirements-infographic-bulletin-3-26-21.pdf (accessed September 27, 2023).

4) Shimada, W.; Shiro, M.; Kondo, H.; Takeya, S.; Oyama, H.; Ebinuma, T.; Narita, H. Tetra-*n*-butylammonium bromide-water (1/ 38). *Acta Crystallogr., Sect. C: Cryst. Struct. Commun*. **2005**, *C61*, o65−o66. DOI: 10.1107/S0108270104032743

5) Rodionova, T.; Komarov, V.; Villevald, G.; Aladko, L.; Karpova, T.; Manakov, A. Calorimetric and Structural Studies of Tetrabutylammonium Chloride Ionic Clathrate Hydrates. *J. Phys. Chem*. *B* **2010**, *114*, 11838–11846. DOI: 10.1021/jp103939q

6) Rodionova, T. V.; Komarov, V. Y.; Villevald, G. V.; Karpova, T. D.; Kuratieva, N. V.; Manakov, A. Y. Calorimetric and Structural Studies of Tetrabutylammonium Bromide Ionic Clathrate Hydrates. *J. Phys. Chem. B* **2013**, *117*, 10677−10685. DOI: 10.1021/jp406082z

7) Muromachi, S.; Takeya, S.; Yamamoto, Y.; Ohmura, R. Characterization of tetra-*n*-butylphosphonium bromide semiclathrate hydrate by crystal structure analysis. *CrystEngComm* **2014**, *16*, 2056−2060. DOI: 10.1039/C3CE41942H

8) Sugahara, T.; Machida, H. Dissociation and nucleation of tetra-*n*-butyl ammonium bromide semi-clathrate hydrates at high pressure. *J. Chem. Eng. Data* **2017***,* **62**, 2721−2725. DOI: 10.1021/acs.jced.7b00115

9) Ogoshi, H.; Takao, S. Air-Conditioning System Using Clathrate Hydrate Slurry. *JFE Technical Report* **2004**, *3*, 1−5.

10) Dyadin, Y. A.; Gaponenko, L. A.; Aladko, L. S.; Bogatyryova, S. V. Clathrate Hydrate of Tetrabutylammonium Carboxylates and Dicarboxylates. *J. Incl. Phenom.* **1984**, *2*, 259−266. DOI: 10.1007/BF00663264

11) Shimada, J.; Shimada, M.; Sugahara, T.; Tsunashima, K.; Tani, A.; Tsuchida, Y.; Matsumiya, M. Phase Equilibrium Relations of Semiclathrate Hydrates Based on Tetra-*n*-butylphosphonium Formate, Acetate, and Lactate, *J. Chem. Eng. Data* **2018**, *63*, 3615 − 3620. DOI: 10.1021/acs.jced.8b00481

12) Azuma, S.; Shimada, J.; Tsunashima, K.; Sugahara, T.; Tani, A.; Hirai, T. Equilibrium Phase Relations and Dissociation Enthalpies of Tri-*n*-butylalkenylphosphonium Bromide Semiclathrate Hydrates. *J. Chem. Eng. Data* **2022**, *67*, 1415−1420. DOI: 10.1021/acs.jced.2c00146

13) Shimada, J.; Yamada, M.; Tani, A.; Sugahara, T.; Tsunashima, K.; Tsuchida, Y.; Hirai, T. Thermodynamic Properties of Tetra-*n*-butylphosphonium Dicarboxylate Semiclathrate Hydrates, *J. Chem. Eng. Data* **2022**, *67*, 67−73. DOI: 10.1021/acs.jced.1c00741

14) Nakayama, H.; Watanabe, K. Hydrates of Organic Compounds. II. The Effect of Alkyl Groups on the Formation of Quaternary Ammonium Fluoride Hydrates. *Bull. Chem. Soc. Jpn* **1976**, *49*, 1254−1256. DOI: 10.1246/bcsj.49.1254

15) Sakamoto, H.; Sato, K.; Shiraiwa, K.; Takeya, S.; Nakajima, M.; Ohmura, R. Synthesis, characterization and thermal-property measurements of ionic semi-clathrate hydrates formed with tetrabutylphosphonium chloride and tetrabutylammonium acrylate. *RSC Adv.*, **2011**, *1*, 315−322. DOI: 10.1039/C1RA00108F

16) Oshima, M.; Kida, M.; Jin, Y.; Nagao, J. Dissociation behaviour of (tetra-*n*-butylammonium bromide + tetra-*n*-butylammonium chloride) mixed semiclathrate hydrate systems. *J. Chem. Thermodyn.* **2015**, *90*, 277−281. DOI: 10.1016/j.jct.2015.07.009

17) Muromachi, S.; Takeya, S. Design of thermophysical properties of semiclathrate hydrates formed by tetra-*n*-butylammonium hydroxybutyrate. *Ind. Eng. Chem. Res.* **2018**, *57*, 3059−3064. DOI: 10.1021/acs.iecr.7b05028

18) Arai, Y.; Koyama, R.; Endo, F.; Hotta, A.; Ohmura, R. Thermophysical property measurements on tetrabutylphosphonium sulfate ionic semiclathrate hydrate consisting of the bivalent anion. *J. Chem. Thermodyn*. **2019**, *131*, 330−335. DOI: 10.1016/j.jct.2018.11.017

19) Shimada, J.; Shimada, M.; Sugahara, T.; Tsunashima, K.; Tani, A.; Tsuchida, Y.; Matsumiya, M. Phase equilibrium relations of tetra-*n*-butylphosphonium propionate and butyrate semiclathrate hydrates. *Fluid Phase Equilib.* **2019**, *485*, 61−66. DOI: 10.1016/j.fluid.2018.11.038

20) Koyama, R.; Hotta, A.; Ohmura, R. Equilibrium temperature and dissociation heat of tetrabutylphosphonium acrylate (TBPAc) ionic semi-clathrate hydrate as a medium for the hydrate-based thermal energy storage system. *J. Chem. Thermodyn*. **2020**, *144*, 106088. DOI: 10.1016/j.jct.2020.106088

21) Miyamoto, T.; Koyama, R.; Kurokawa, N.; Hotta, A.; Alavi, S.; Ohmura, R. Thermophysical Property Measurements of Tetrabutylphosphonium Oxalate (TBPOx) Ionic Semiclathrate Hydrate as a Media for the Thermal Energy Storage System. *Front. Chem*. **2020**, *8*, 547. DOI: 10.3389/fchem.2020.00547

22) Shimada, J.; Shimada, M.; Sugahara, T.; Tsunashima, K.; Takaoka, Y.; Tani, A. Phase equilibrium temperature and dissociation enthalpy in the tri-*n*-butylalkylphosphonium bromide semiclathrate hydrate systems. *Chem. Eng. Sci*. **2021**, *236*, 116514. DOI: 10.1016/j.ces.2021.116514

23) Azuma, S.; Shimada, J.; Tsunashima, K.; Sugahara, T.; Hirai, T. Effect of introducing a cyclobutylmethyl group into an onion cation on the thermodynamic properties of ionic clathrate hydrate, *New J. Chem*. **2023**, *47*, 231−237. DOI: 10.1039/D2NJ04361K

24) Yamamoto, K.; Iwai, T.; Hiraga, K.; Miyamoto, T.; Hotta, A.; Ohmura R. Synthesis and thermophysical properties of Tetrabutylammonium picolinate hydrate as an energy storage phase change materials for cold chain. *J. Energy Storage* **2022**, *55*, 105812. DOI: 10.1016/j.est.2022.105812

25) Chen, D.; Jiang, J.; Kim, G.-H.; Yang, C.; Pesaran, A. Comparison of different cooling methods for lithium ion battery cells, *Appl. Therm. Eng.* **2016**, *94*, 846 − 854. DOI: 10.1016/j.applthermaleng.2015.10.015

26) Nakayama, H.; Watanabe, K. Hydrates of Organic Compounds. III. The formation of Clathrate-like Hydrates of Tetrabutylammonium Dicarboxylates. *Bull. Chem. Soc. Jpn* **1978**, *51*, 2518−2522. DOI: 10.1246/bcsj.51.2518

27) Dyadin, Y.A.; Udachin, K.A. Clathrate polyhydrates of peralkylonium salts and their analogs. *J. Struct. Chem*. **1987**, *28*, 394−432. DOI: 10.1007/BF00753818

28) Muromachi, S.; Abe, T.; Yamamoto, Y.; Takeya, S. Hydration structures of lactic acid: characterization of the ionic clathrate hydrate formed with a biological organic acid anion. *Phys. Chem. Chem. Phys.*, **2014**, *16*, 21467−21472. DOI: 10.1039/C4CP03444A

29) Muromachi, S.; Kamo, R.; Abe, T.; Hiaki, T.; Takeya, S. Thermodynamic stabilization of semiclathrate hydrates by hydrophilic group. *RSC Adv.*, **2017**, *7*, 13590 − 13594. DOI: 10.1039/C7RA01048F

30) Yin, Z.; Zheng, J.: Kim, H.; Seo, Y.; Linga, P. Hydrates for cold energy storage and transport: A review, *Advances in Applied Energy* **2021**, *2*, 100022. DOI: 10.1016/j.adapen.2021.100022

31) Sugahara, T.; Machida, H.; Muromachi, S.; Tenma, N. Thermodynamic properties of tetra-*n*-butylammonium 2-ethylbutyrate semiclathrate hydrate for latent heat storage. *Int. J. Refrig.* **2019**, *106*, 113−119. DOI: 10.1016/j.ijrefrig.2019.06.029

32) Shimada, J.; Shimada, M.; Azuma, S.; Sugahara, T.; Tsunashima, K.; Hirai, T. Peritectic phase behavior of tetra-*n*-butylphosphonium trifluoroacetate semiclathrate hydrate. *Fluid Phase Equilib.* **2023**, *563*, 113727. DOI: 10.1016/j.fluid.2023.113727

33) Delahaye, A.; Fournaison, L.; Marinhas, S.; Chatti, I.; Petitet, J.-P.; Dalmazzone, D.; Fürst, W. Effect of THF on Equilibrium Pressure and Dissociation Enthalpy of CO_2 Hydrates Applied to Secondary Refrigeration, *Ind. Eng. Chem. Res.* **2006**, *45*, 391−397. DOI: 10.1021/ie050356p

34) Chekcell; https://www.ccp14.ac.uk. Chekcell developed by L. Laugier and B. Bochu, Laboratoire des Materiaux et du Genie Physique, Ecole Superieure de Physique de Grenoble: Grenoble, France (accessed September 27, 2023).

35) Dong, C. PowderX: Windows-95-based Program for Powder X-ray Diffraction Data Processing, *J. Appl. Crystallogr.* **1999**, *32*, 838. DOI: 10.1107/S0021889899003039

36) Muromachi, S.; Takeya, S. Thermodynamic Properties and Crystallographic Characterization of Semiclathrate Hydrates Formed with Tetra-*n*-butylammonium Glycolate. *ACS Omega* **2019**, *4*, 7317−7322. DOI: 10.1021/acsomega.9b00422

TOC

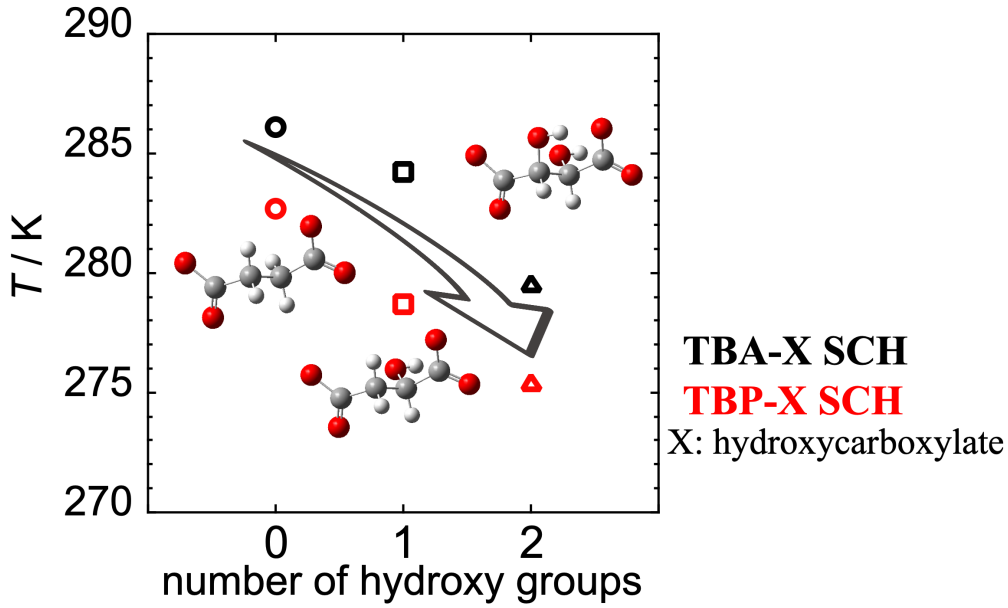
290
285
280
275
270
T / K
0
1
2
number of hydroxy groups
TBA-X SCH
TBP-X SCH
X: hydroxycarboxylate